Finite Control-Set Model Predictive Control (FCS-MPC) of Nested Neutral Point-Clamped (NNPC) Converter

Mehdi Narimani, *Member, IEEE*, Bin Wu, *Fellow, IEEE*, Venkata Yaramasu, *Member, IEEE*, Zhongyuan Cheng, *Member, IEEE*, and Navid Reza Zargari, *Senior Member, IEEE*

***Abstract*—This paper proposes a model predictive control (MPC) strategy for a nested neutral point-clamped (NNPC) converter to control output currents and voltages of flying capacitors. The NNPC converter is a four-level converter topology for medium-voltage applications with interesting properties such as operating over a wide range of voltages (2.4–7.2 KV) without the need for connecting power semiconductor in series, high quality output voltage, less number of components compared to other classical four-level topologies. A discrete-time model of the converter is presented and all the control objectives are formulated in terms of the switching states. During each sampling interval, the predicted variables are assessed by the cost function and the best switching state which gives minimum value for the cost function is selected and applied to the converter gating terminals. The performances of the NNPC converter and predictive control scheme are verified through MATLAB/Simulink simulations and their feasibility is evaluated experimentally.**

***Index Terms*—DC–AC power conversion, finite control-set model predictive control (FCS-MPC), multilevel converter.**

I. Introduction

MULTILEVEL voltage source converters (VSCs) are suitable candidates for high-power and medium-voltage (MV) applications. The main features of these configurations, as compared with the two-level VSC, are their capabilities to reduce: a) harmonic distortion of the ac-side waveforms, b) *dv/dt* switching stresses, c) switching losses, and d) minimize or even eliminate the interface transformer [1]–[5]. In addition to standard multilevel converters such as neutral point-clamped (NPC), flying capacitor (FC), and the cascaded H-bridge; a number of variants and new multilevel converters have been proposed in the literature [6]–[16]. Among all of these multilevel converters, the four-level NNPC converter [16], shown in Fig. 1, has many interesting properties such as operating over a wide range of voltages (2.4–7.2 KV) without the need for connecting power semiconductor devices in series, equal voltage stress for all the switches (one-third of the dc voltage), less number of components in comparison to the other four-level converters.

The MV NNPC converter is suitable for many applications such as: STATCOM, train traction, ship propulsion, regenerative conveyors, wind and photovoltaic energy conversion systems, and general MV motor drive applications (pumps, fans, etc.) [1]. In these applications, there are two main important issues for an NNPC converter: control of output currents and FC voltages.

The finite control set model predictive control (FCS-MPC) has recently emerged as a new control tool in power electronics and drives. This scheme offers a conceptually different approach to control the power converters while eliminating the need for linear regulators and SVM/PWM modulators [17]. In this approach, the control goals are expressed as a cost function and its minimization is used as a criterion to choose the best switching state which would be applied to the converter during next sampling interval.

In this paper, a FCS-MPC strategy is proposed to control the NNPC converter. The discrete-time model of the load currents and FC voltages is presented. The future behavior of the control variables for all the possible switching states has been obtained. A cost function is defined to assess the predicted variables. The switching state which minimizes the cost function value is selected and applied to the converter directly. The performance of the control scheme is verified by simulation and experimental results.

II. Predictive Control of the NNPC Converter

A. Operation of the NNPC Converter

The NNPC topology, as shown in Fig. 1, is a combination of a FC topology and a neutral point-clamped (NPC) topology named NNPC converter which provides a four-level output voltage. To ensure equally spaced steps in the output voltages, the capacitor Cx_1 and Cx_2, $x = a, b, c$ are charged and should be maintained at one-third of the total dc-link voltage.

Four output levels can be achieved from the six distinct switching combinations. The list of switching combinations is shown in Table II. It should be noted that all switch devices are rated for one-third of the dc-link voltage. Another advantage of the NNPC converter is the redundancy in switch combination to produce output levels. For example, two redundant switching

Manuscript received September 4, 2014; revised December 1, 2014; accepted January 13, 2015. Date of publication January 23, 2015; date of current version August 21, 2015. Recommended for publication by Associate Editor Prof. K.-B. Lee.

M. Narimani is with the Department of Electrical and Computer Engineering, Ryerson University, Toronto, ON M5B 2K3, Canada, and also with Rockwell Automation Canada, Cambridge, ON N1R5X1 Canada (e-mail: mnariman@gmail.com;).

B. Wu and V. Yaramasu are with the Department of Electrical and Computer Engineering, Ryerson University, Toronto, ON M5B 2K3 Canada (e-mail: bwu@ee.ryerson.ca; vyaramas@ee.ryerson.ca).

Z. Cheng and N. R. Zargari are with the Department of Medium Voltage Research and Development, Rockwell Automation Canada, Cambridge, ON N1R5X1 Canada (e-mail: gcheng@ra.rockwell.com; nrzargari@ra.rockwell.com).

Color versions of one or more of the figures in this paper are available online at http://ieeexplore.ieee.org.

Digital Object Identifier 10.1109/TPEL.2015.2396033

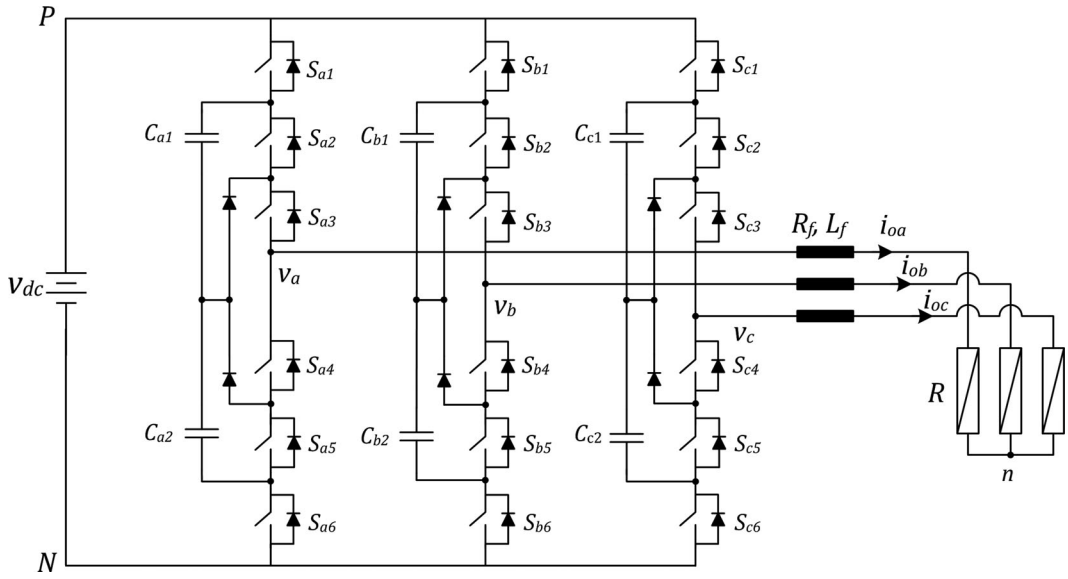

Fig. 1 NNPC converter.

TABLE I
SWITCHING STATES OF THE FOUR-LEVEL NNPC AND CONTRIBUTION OF THE AC-SIDE CURRENTS TO THE FC VOLTAGES

S_{x1}	S_{x2}	S_{x3}	S_{x4}	S_{x5}	S_{x6}	v_x	v_{Cx1}	v_{Cx2}
1	1	1	0	0	0	$v_{\rm dc}$	No Impact	No Impact
1	0	1	1	0	0		Charging ($i_{ox} > 0$) Discharging ($i_{ox} < 0$)	No Impact
0	1	1	0	0	1	$\frac{2v_{\rm dc}}{3}$	Discharging ($i_{ox} > 0$) Charging ($i_{ox} < 0$)	Discharging ($i_{ox} > 0$) Charging ($i_{ox} < 0$)
1	0	0	1	1	0	$\frac{v_{\rm dc}}{3}$	Charging ($i_{ox} > 0$) Discharging ($i_{ox} < 0$)	Charging ($i_{ox} > 0$) Discharging ($i_{ox} < 0$)
0	0	1	1	0	1		No Impact	Discharging ($i_{ox} > 0$) Charging ($i_{ox} < 0$)
0	0	0	1	1	1	0	No Impact	No Impact

states (as can be seen in Table I) are able to generate voltage levels of $2/3v_{\rm dc}$ and $1/3v_{\rm dc}$. Each redundant state provides a specific charging and discharging current path for each FC. This is a specific feature of redundant switching states that can be used to achieve voltage balancing of the capacitors. The main technical challenge is to identify the best redundant switching state to achieve this.

B. Mathematical Model of the NNPC Converter

The FCS-MPC approach is an optimization algorithm that eliminates the need for linear regulators and can be easily implemented on the current digital control platforms. This method requires the discrete-time model of the converter and load. In this section, the mathematical model of the NNPC converter is explained.

In order to perform the optimization algorithm and select the optimal control action, all the control variables should be expressed in terms of measured quantities, parameters of the system, and switching states of the converter.

1) Model of Load Currents: Referring to Table II, the voltage in any phase *x* of the NNPC inverter with respect to the negative point of the dc-link *N* can be expressed in terms of switching states and FC voltages as follows:

TABLE II
POSSIBLE SWITCHING STATES OF THE NNPC CONVERTER WHEN ($x = a, b, c$)

S_{x1}	S_{x2}	S_{x3}	S_{x4}	S_{x5}	S_{x6}	v_x
1	1	1	0	0	0	$v_{\rm dc}$
1	0	1	1	0	0	$v_{\rm dc} - v_{cx1}$
0	1	1	0	0	1	$v_{cx1} + v_{cx2}$
1	0	0	1	1	0	$v_{\rm dc} - v_{cx1} - v_{cx2}$
0	0	1	1	0	1	v_{cx2}
0	0	0	1	1	1	0

$$\begin{aligned} v_{xN} =\ & S_{x1}v_{\rm dc} + (S_{x2}-1)v_{Cx1} \\ & + (S_{x3}-1)v_{Cx2} + (1-S_{x1})(v_{Cx1}+v_{Cx2}) \\ x =\ & a, b, c \end{aligned} \tag{1}$$

where v_{cx1} and v_{cx2} are the FC voltages for phase *x*.

By applying Kirchhoff's voltage law to Fig. 1, the inverter voltages can be expressed in terms of load currents as follows:

$$\begin{aligned} v_{aN} &= (R_{fa}+R_a)i_{oa} + L_{fa}\frac{di_{oa}}{dt} + v_{nN} \\ v_{bN} &= (R_{fb}+R_b)i_{ob} + L_{fb}\frac{di_{ob}}{dt} + v_{nN} \\ v_{cN} &= (R_{fc}+R_c)i_{oc} + L_{fc}\frac{di_{oc}}{dt} + v_{nN} \end{aligned} \tag{2}$$

where R_{fa}, R_{fb}, and R_{fc} are filter leakage resistances of phases *a*, *b*, and *c*, respectively. L_{fa}, L_{fb}, and L_{fc} are filter inductances of phases *a*, *b*, and *c*, respectively. R_a, R_b, and R_c are load resistances of phases *a*, *b*, and *c*, respectively. i_{oa}, i_{ob}, and i_{oc} are load currents of phases *a*, *b*, and *c*, respectively. v_{nN} is the voltage between load neutral and negative dc-rail

$$\begin{aligned} v_{nN} &= \frac{1}{3}(v_{aN}+v_{bN}+v_{cN}) \\ v_{xn} &= v_{xN} - v_{nN} \\ x &= a,b,c. \end{aligned} \tag{3}$$

The expression (2) can be simplified to

$$\mathbf{v_o} = (R_f + R)\mathbf{i_o} + L_f\frac{\mathrm{d}\mathbf{i_o}}{\mathrm{dt}} \tag{4}$$

where

$$\begin{aligned} \mathbf{v_o} &= \begin{bmatrix} v_{an} & v_{bn} & v_{cn} \end{bmatrix}^T \\ \mathbf{i_o} &= \begin{bmatrix} i_{oa} & i_{ob} & i_{oc} \end{bmatrix}^T \\ R_f &= R_{fa} = R_{fb} = R_{fc} \\ L_f &= L_{fa} = L_{fb} = L_{fc} \\ R &= R_a = R_b = R_c. \end{aligned} \tag{5}$$

The continuous-time expression for the load current can be derived from (4) as

$$\frac{d\mathbf{i_o}}{dt} = \frac{1}{L_f}\left[\mathbf{v_o} - (R_f + R)\mathbf{i_o}\right]. \tag{6}$$

To implement the control algorithm in the microprocessor-based hardware, the continuous-time model should be converted to discrete time. In this paper, the backward Euler method is considered to approximate the first-order derivative given in (7). This is demonstrated as follows:

$$\frac{di_o}{dt} = \frac{\mathrm{i_o}\,(k+1) - \mathrm{i_o}(k)}{T_s} \tag{7}$$

where T_s is the sampling time. By substituting (7) into (6) and shifting into one future sample, the discrete-time model of the output current can be obtained as [18]

$$\mathbf{i_o}\,(k+1) = K_v\ \mathbf{v_o}\,(k+1) + K_i\ \mathbf{i_o}\,(k) \tag{8}$$

where

$$\begin{aligned} K_v &= \frac{T_s}{L_f + (R_f+R)T_s} \\ K_i &= \frac{L_f}{L_f + (R_f+R)T_s}. \end{aligned} \tag{9}$$

Equation (8) shows that the output current prediction in $(k+1)$ requires the measured load current value and the predicted converter output load voltage. The prediction of the load voltage uses the 216 (6^3) possible switching states and the measured FC voltages (see (1)).

2) Model of FC Voltages: The voltages of FCs should be regulated in the NNPC to ensure equally spaced steps in the output voltages, otherwise the semiconductor device voltage stress increases. In this section, the model of FC voltages is presented in terms of the NNPC switching states

$$\begin{aligned} v_{Cx1}\,(t) &= v_{Cx1}\,(0) + \int_{0+}^{t} i_{Cx1}\,(\tau)\,d\tau \\ v_{Cx2}\,(t) &= v_{Cx2}\,(0) + \int_{0+}^{t} i_{Cx2}\,(\tau)\,d\tau \\ x &= a,b,c. \end{aligned} \tag{10}$$

Referring to Table I, the capacitor currents are directly related to the three-phase output currents as follows:

$$\begin{aligned} i_{Cx1} &= (S_{x1} - S_{x2})\,.\,i_{ox} \\ i_{Cx2} &= (S_{x5} - S_{x6})\,.\,i_{ox} \\ x &= a,b,c. \end{aligned} \tag{11}$$

The discrete-time model for FC voltages can be obtained from (10) as

$$\begin{aligned} v_{Cx1}\,(k+1) &= v_{Cx1}\,(k) + \frac{T_s}{C_{x1}} i_{Cx1}\,(k) \\ v_{Cx2}\,(k+1) &= v_{Cx2}\,(k) + \frac{T_s}{C_{x2}} i_{Cx2}\,(k) \\ x &= a,b,c \end{aligned} \tag{12}$$

where

$$\begin{aligned} i_{Cx1}\,(k) &= (S_{x1} - S_{x2})\,.\,i_{ox}(k) \\ i_{Cx2}\,(k) &= (S_{x5} - S_{x6})\,.\,i_{ox}(k) \\ x &= a,b,c. \end{aligned} \tag{13}$$

C. Model Predictive Current Control of the NNPC Converter

The proposed predictive current control scheme is shown in Fig. 2. It uses the discrete-time model to predict the future behavior of the variables to be controlled. The predictive control consists of the following steps:

1) *Measurements:* As a first step in the implementation, the FC voltages and load current are measured at *k*th instant.
2) *References calculation:* The reference load current values are obtained based on the application employing the NNPC converter. For example, in the grid-connected applications in wind and photovoltaic energy systems, the references are generated such that grid-side active and reactive power can be controlled. In motor drives, the reference currents are generated to regulate the torque and speed of the machine. In order to keep the generality of the paper, the references are chosen as user defined. Since the cost function performs the comparison in $(k+1)$

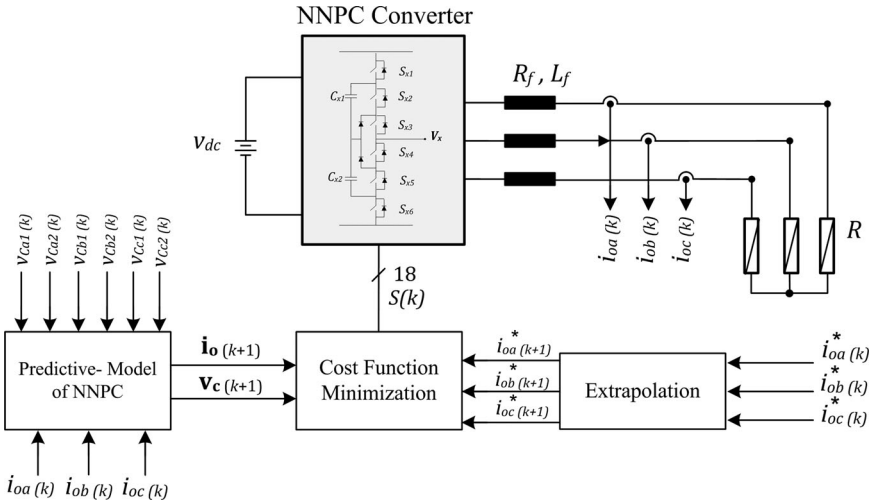

Fig. 2 Proposed MPC control scheme for an NNPC converter.

sampling instant, the references should be extrapolated to future state. The following fourth-order Lagrange extrapolation [19] is used here

$$\mathbf{i}^*_{\mathbf{o}}(k+1) = 4\,\mathbf{i}^*_{\mathbf{o}}(k) - 6\,\mathbf{i}^*_{\mathbf{o}}(k-1) + 4\,\mathbf{i}^*_{\mathbf{o}}(k-2) - \mathbf{i}^*_{\mathbf{o}}(k-3). \quad (14)$$

3) *Prediction of output currents and FC voltages:* The predictive model of the NNPC converter given in (8)-(13) uses the measured capacitor voltages and load currents at *k*th instant to predict the output currents and FC voltages at time $(k+1)$.
4) *Cost function optimization:* A cost function is defined with two control objectives. The first one is to minimize the error between the predicted load currents $\mathbf{i_o}(k+1)$ and their references $\mathbf{i^*_o}(k+1)$, and the second one is to regulate the FC voltages. These control objectives are represented as follows:

$$\begin{aligned} g_{\text{track}}(k+1) &= \sum_{x=a,b,c} \left[i^*_{ox}(k+1) - i_{ox}(k+1)\right]^2 \\ g_{\text{cap}}(k+1) &= \lambda_{\text{cap}} \cdot \sum_{x=a,b,c} \left\{ \sum_{i=1}^{2} \left[v^*_{cx} - v_{cxi}(k+1)\right]^2 \right\} \end{aligned} \quad (15)$$

where λ_{cap} is the weighting factor and

$$v^*_{cx} = \frac{1}{3} v_{\text{dc}}. \quad (16)$$

To calculate the weighting factor to control the capacitor voltages, the following equation has been employed:

$$\lambda_{\text{cap}} = \frac{i_{o,n}}{v^*_{cx}} \quad (17)$$

where $i_{o,n}$ is the nominal (rated) output current and v^*_{cx} is the reference value of the FC voltages.

The importance of the capacitor voltages balancing can be substantiated with the main objective of load currents regulation by the weighting factor λ_{cap}. The final cost function is defined as follows by combining the above two sub cost functions:

$$g(k+1) = g_{\text{track}}(k+1) + g_{\text{cap}}(k+1). \quad (18)$$

The main objective for the control algorithm is to achieve the cost function values close to zero. During each sampling interval, 216 predictions obtained for the load current are compared with its extrapolated reference. Similarly, the 216 predictions for each capacitor voltage are used by the cost function. The switching state which produces minimum value for the cost function during *k*th instant is selected and applied during the next sampling interval.

III. Simulation Results

In order to show the performance of the proposed FCS-MPC strategy for the NNPC four-level converter, simulation studies have been carried out in MATLAB/Simulink environment for a 5-MVA/7.2-kV converter. The parameters of the system are shown in Table III. The effectiveness of the predictive controller to generate output voltages, regulate load currents, and control voltage of FCs is analyzed during both steady-state and transient interval.

A. Steady-State Analysis

Fig. 3 shows the reference current, the predicted current, and the output current in a half cycle that shows output current can follow the predicted current. Fig. 4 shows the simulation results in the steady state with balanced references ($i^*_{oa} = i^*_{ob} = i^*_{oc} = 340\ A = 0.85$ p.u. at 60 Hz) and balanced loads ($R_a = R_b = R_c = 10\ \Omega = 1$ p.u.) for a sampling time of $T_s = 50\ \mu$s. According to (17), the weighting factor λ_{cap} is calculated which is equal to 0.1. Both reference currents and output currents are shown in Fig. 4. The voltage of FCs in the steady-state condition is shown in Fig. 5.

TABLE III
PARAMETERS OF THE STUDY SYSTEM (SIMULATION)

Converter parameters	Values	Values (p.u)
Converter rating	5 MVA	1.0
Output voltage	7.2 kV	1.0
Flying capacitors	1000 μF	4.0
Input dc voltage	12.5 kV	–
Output frequency	60 Hz	1.0
Output inductance	5.5mH	0.2
Output load	10 Ω	1.0

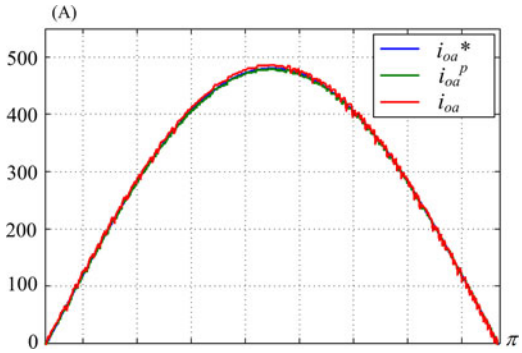

Fig. 3 Reference current, predictive current, and output current.

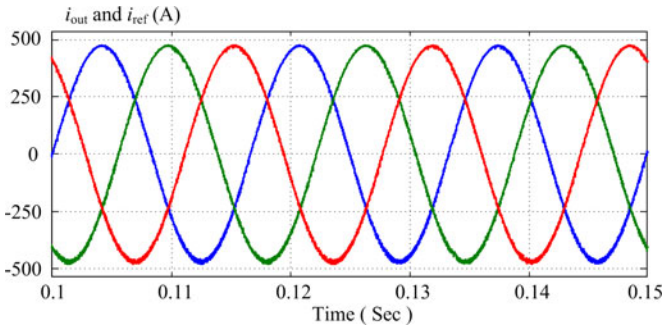

Fig. 4 Reference currents and output currents; steady-state simulation.

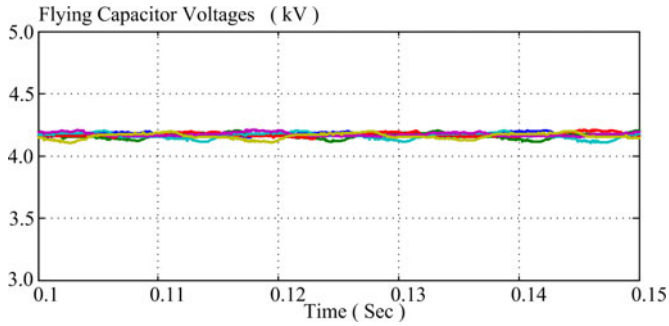

Fig. 5 FC voltages; steady-state simulation.

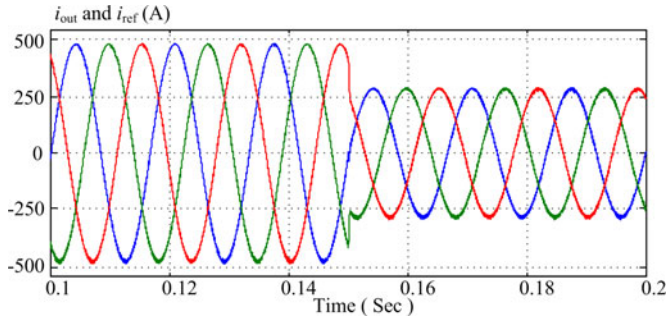

Fig. 6 Reference currents and output currents; step changes in reference currents from 340 A (0.85 p.u.) to 200 A (0.5 p.u.).

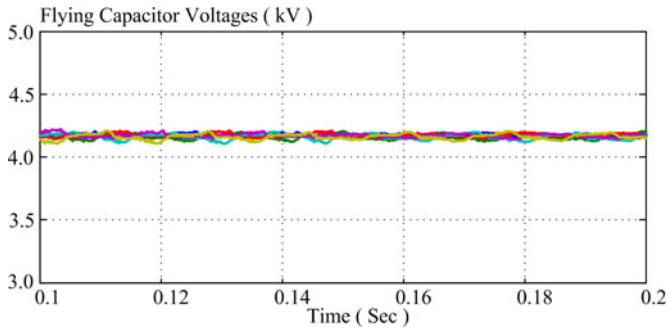

Fig. 7 FC voltages; step changes in reference currents from 340 A (0.85 p.u.) to 200 A (0.5 p.u.).

B. Transient-State Analysis

Transient analysis is carried out with the sampling time $T_s = 50$ μs and the output frequency 60 Hz. The load is considered to be $R_a = R_b = R_c = 10\ \Omega$. Step change from $i_{oa}^* = i_{ob}^* = i_{oc}^* = 340$ A $= 0.85$ p.u. to $i_{oa}^* = i_{ob}^* = i_{oc}^* = 200$ A $= 0.5$ p.u. is applied. Fig. 6 shows the simulation results when step change in the reference input has been applied at $t = 0.15$ s. Fig. 7 shows the voltage of FCs during the transient state. Figs. 6 and 7 show that the currents can track the references well and voltages of the capacitors are well regulated.

C. Dynamic Behavior of the Capacitor Voltages

To show the dynamic behavior of the FCs, assume that the NNPC converter is operating in normal condition and suddenly at $t = 0.15$ s, the control of the FC voltage is deactivated ($\lambda_{\rm cap} = 0$) and at $t = 0.3$ s the capacitor voltage controller reactivated again ($\lambda_{\rm cap} = 0.1$). Fig. 8 shows that when the controller is deactivated, the capacitors start diverging and when the controller reactivates the capacitor voltages converge to nominal values.

D. Performance Comparison Between FCS-MPC and the Classic Controller for the NNPC Converter

To compare the performance of the FCS-MPC strategy, a classic current controller (PI) with the SPWM scheme has been developed for the NNPC converter. The SPWM scheme is the strategy presented in [20] and the simulation parameters are the same as shown in Table III. Fig. 9 shows the output current and the reference current for one phase. Comparison between Figs. 6 and 9 shows that the dynamic response of the FCS-MPC strategy is much improved. In Fig. 6, when the reference current

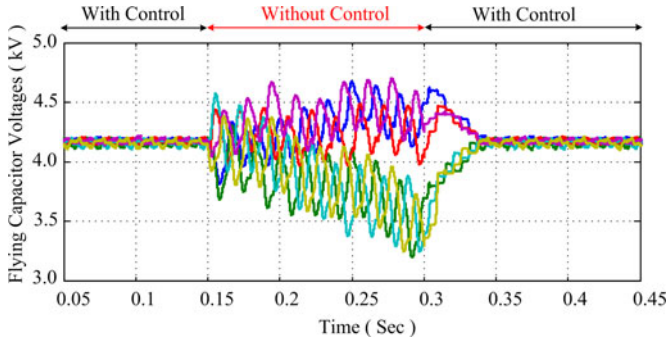

Fig. 8 Dynamic performance of the capacitor voltages.

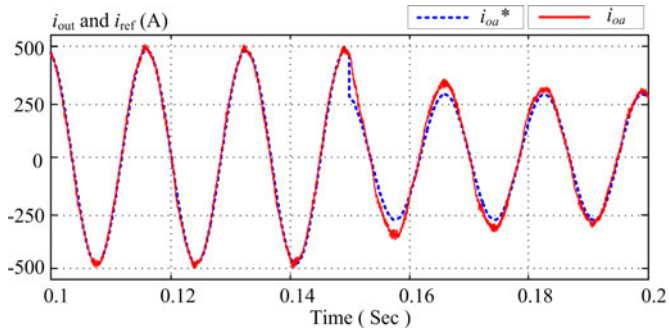

Fig. 9 Reference current and output current with SPWM scheme and PI controller; step changes in reference currents from 340 A (0.85 p.u.) to 200 A (0.5 p.u.).

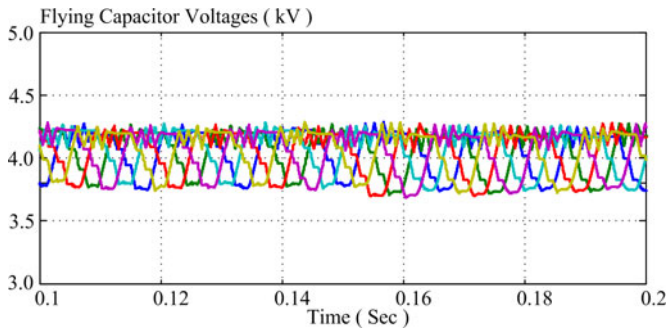

Fig. 10 FC voltages with SPWM scheme and PI controller; step changes in reference currents from 340 A (0.85 p.u.) to 200 A (0.5 p.u.).

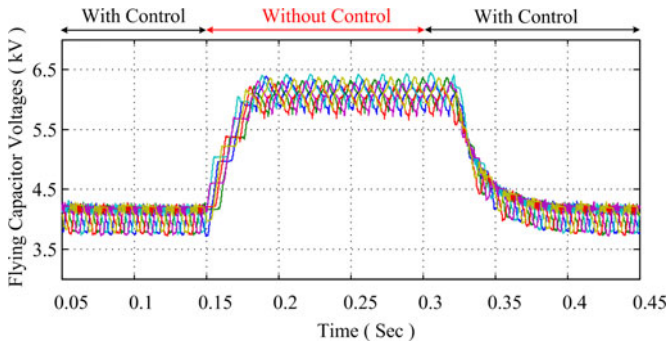

Fig. 11 Dynamic performance of the capacitor voltages with SPWM scheme and PI controller.

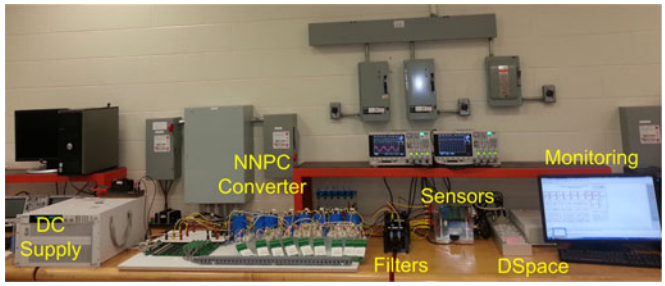

Fig. 12 Experimental setup for the NNPC converter.

TABLE IV
PARAMETERS OF THE STUDY SYSTEM (EXPERIMENTAL)

Converter Parameters	Values
Converter rating	5 kVA
Flying capacitors	1000 μF
Input dc voltage	400 V
Output frequency	60 Hz
Output inductor	5 mH
Output load	10 Ω

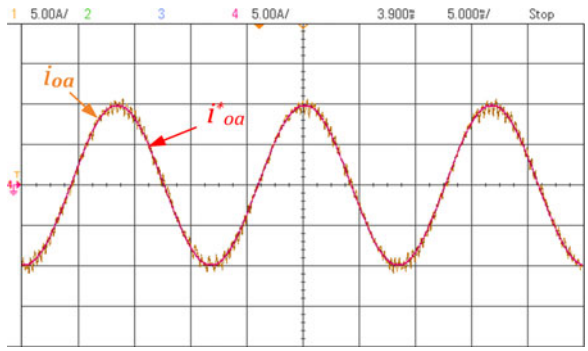

Fig. 13 Experimental results, steady-state predictive current, and output current.

changes, the output current will change almost instantly; while in Fig. 9 it takes about two cycle for output current to track the reference current. Fig. 10 shows FC voltages, which with SPWM strategy the voltage ripple are almost four times the FCS-MPC strategy.

Fig. 11 shows the FC voltages with and without controller and as can be compared to Fig. 8, the dynamic behavior of the FC has been improved by FCS-MPC strategy.

IV. EXPERIMENTAL RESULTS

The feasibility of the proposed converter is evaluated experimentally. Fig. 12 shows the experimental setup for the proposed NNPC converter. The parameters of Table IV were used for experiments as a scaled-down prototype.

Figs. 13–15 show the performance of the proposed converter under the steady-state operation. Fig. 13 shows the inverter reference current, the predictive current, and the output current for phase a. Fig. 14 shows the output currents of the inverter in the steady-state operation, and Fig. 14 shows the voltage of FCs when the reference currents are $i^*_{oa} = i^*_{ob} = i^*_{oc} = 10$ A and R_a

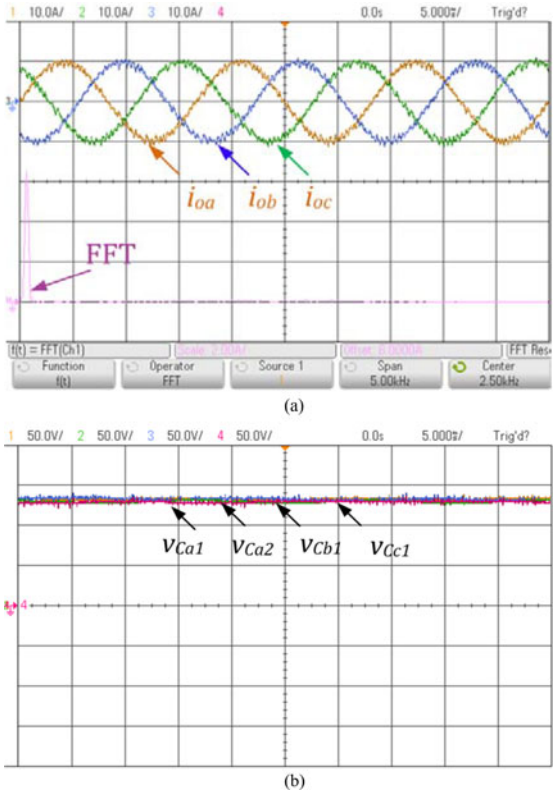

Fig. 14 Experimental results, steady state: a) output currents and FFT of phase a and b) voltages of FCs, $\mathrm{m} = 0.9$, $\mathrm{PF} = 0.9$.

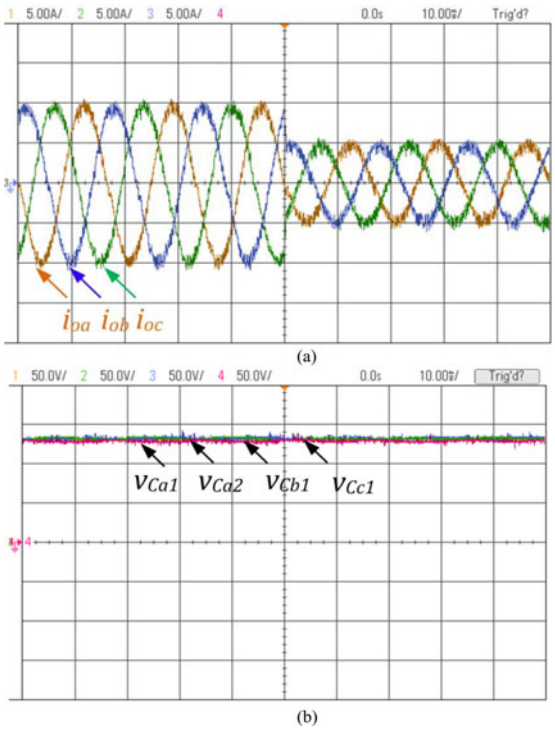

Fig. 15 Experimental results, transient state, step change in reference currents from 10 to 5 A: a) output currents and b) voltages of FCs.

$= R_b = R_c = 10\ \Omega$. Fig. 15 shows the performance of the proposed MPC for the NNPC converter under transient condition when reference currents change from $i^*_{oa} = i^*_{ob} = i^*_{oc} = 10$ A to $i^*_{oa} = i^*_{ob} = i^*_{oc} = 5$ A.

V. Conclusion

An FCS-MPC strategy for an NNPC converter is proposed. A discrete-time model of the converters is presented, and all the control objectives are formulated in terms of the switching states. The load currents and FC voltages are regulated during each sampling interval with the help of the cost function. The best switching state which minimizes the cost function is selected and applied to the converter. The requirements for the linear PI regulators and complex modulation stage have been eliminated. The simulation and experimental results are in a close relation and they validate the proposed control technique and power converter.

References

[1] S. Kouro, M. Malinowski, K. Gopakumar, J. Pou, L. G. Franquelo, B. Wu, J. Rodriguez, M. A. Perez, and J. I. Leon, "Recent advances and industrial applications of multilevel converters," *IEEE Trans. Ind. Electron.*, vol. 57, no. 8, pp. 2553–2580, Aug. 2010.

[2] B. Wu, *High-Power Converters and AC Drives*. Piscataway, NJ, USA: IEEE Press, 2006.

[3] J. Rodriguez, J. Lai, and F. Z. Peng, "Multilevel inverters: A survey of topologies, controls, and applications," *IEEE Trans. Ind. Electron.*, vol. 49, no. 4, pp. 724–738, Aug. 2002.

[4] J. Rodriguez, S. Bernet, B. Wu, J. Pontt, and S. Kouro, "Multilevel voltage source- converter topologies for industrial medium-voltage drives," *IEEE Trans. Ind. Electron.*, vol. 54, no. 6, pp. 2930–2945, Dec. 2007.

[5] M. Saeedifard, P. M. Barbosa, and P. K. Steimer, "Operation and control of a hybrid seven-level converter," *IEEE Trans. Power Electron.*, vol. 27, no. 2, pp. 652–660, Feb. 2012.

[6] Z. Cheng and B. Wu, "A novel switching sequence design for five-level NPC/H-bridge inverters with improved output voltage spectrum and minimized device switching frequency," *IEEE Trans. Power Electron.*, vol. 22, no. 6, pp. 2138–2145, Nov. 2007.

[7] I. Etxeberria-Otadui, A. L. de Heredia, J. San-Sebastian, H. Gaztaaga, U. Viscarret, and M. Caballero, "Analysis of a H-NPC topology for an AC traction front-end converter," in *Proc. 13th EPE-Power Electron. Motion Control Conf.*, Sep. 1–3, 2008, pp. 1555–1561.

[8] V. Guennegues, B. Gollentz, L. Leclere, F. Meibody-Tabar, and S. Rael, "Selective harmonic elimination PWM applied to H-bridge topology in high speed applications," in *Proc. Int. Conf. Power Eng., Energy Electron. Drives*, Mar. 18–20, 2009, pp. 152–156.

[9] S. Choi and M. Saeedifard, "Capacitor voltage balancing of flying capacitor multilevel converters by space vector PWM," *IEEE Trans. Power Del.*, vol. 27, no. 3, pp. 1154–1161, Jul. 2012.

[10] T. Bruckner, S. Bernet, and H. Guldner, "The active NPC converter and its loss-balancing control," *IEEE Trans. Ind. Electron.*, vol. 52, no. 3, pp. 855–868, Jun. 2005.

[11] O. Apeldoorn, B. Odegard, P. Steimer, and S. Bernet, "A 16 MVA ANPC-PEBB with 6 kA IGCTs," in *Proc. IEEE 40th IAS Annu. Meeting Ind. Appl. Conf.*, Oct. 2–6, 2005, vol. 2, pp. 818–824.

[12] J. Meili, S. Ponnaluri, L. Serpa, P. K. Steimer, and J. W. Kolar, "Optimized pulse patterns for the 5-level ANPC converter for high speed high power applications," in *Proc. IEEE 32nd Annu. Conf. Ind. Electron.*, Nov. 6–10, 2006, pp. 2587–2592.

[13] L. A. Serpa, P. M. Barbosa, P. K. Steimer, and J. W. Kolar, "Five level virtual-flux direct power control for the active neutral-point clamped multilevel inverter," in *Proc. IEEE Power Electron. Spec. Conf.*, Jun. 15–19, 2008, pp. 1668–1674.

[14] F. Kieferndorf, M. Basler, L. A. Serpa, J.-H. Fabian, A. Coccia, and G. A. Scheuer, "A new medium voltage drive system based on ANPC-5l technology," in *Proc. IEEE Int. Conf. Ind. Tech.*, Viña del Mar, Chile, Mar. 2010, pp. 605–611.

[15] P. Barbosa, P. Steimer, J. Steinke, L. Meysenc, M. Winkelnkemper, and N. Celanovic, "Active neutral-point-clamped multilevel converters," in *Proc. IEEE 36th Power Electron. Spec. Conf.*, Jun. 16, 2005, pp. 2296–2301.

[16] M. Narimani, B. Wu, G. Cheng, and N. Zargari, "A new nested neutral point clamped (NNPC) converter for medium-voltage (MV) power conversion," *IEEE Trans. Power Electron.*, vol. 29, no. 12, pp. 6375–5382, Dec. 2014.

[17] J. Rodriguez, M. P. Kazmierkowski, J. R. Espinoza, P. Zanchetta, H. Abu-Rub, H. A. Young, and C. A. Rojas, "State of the art of finite control set model predictive control in power electronics," *IEEE Trans. Ind. Inform.*, vol. 9, no. 2, pp. 1003–1016, May 2013.

[18] V. Yaramasu, M. Rivera, M. Narimani, J. Rodriguez, and B. Wu, "Model predictive approach for a simple and effective load voltage control of four-leg inverter with output LC filter," *IEEE Trans. Ind. Electron.*, vol. 61, no. 10, pp. 5259–5270, Jan. 2014.

[19] O.Kukrer, "Discrete-time current control of voltage-fed three-phase PWM inverters," *IEEE Trans. Power Electron.*, vol. 11, no. 2, pp. 260–269, Mar. 1996.

[20] M. Narimani, B. Wu, G. Cheng, and N. Zargari, "A novel and simple single-phase modulator for the nested neutral point clamped (NNPC) converter," submitted for publication, *IEEE Trans. Power Electron.*, DOI: 10.1109/TPEL.2014.2352649, 2014.

Mehdi Narimani (S'09–M'13) received the B.S. and M.S degrees from the Isfahan University of Technology, Isfahan, Iran, in 1999 and 2002, respectively, and the Ph.D. degree from the University of Western Ontario, London, ON, Canada, all in electrical engineering.

He is currently a Postdoctoral Research Associate at the Department of Electrical and Computer Engineering, Ryerson University, Toronto, ON, Canada, and also with Rockwell Automation, Cambridge, ON, Canada. He worked as a faculty member of the Isfahan University of Technology from 2002 to 2009, where he was involved in design and implementation of several industrial projects.

He is the author of more than 45 journal articles, conference proceeding papers, and three patents (pending review). His current research interests include high-power converters, control of power electronics, and renewable energy Systems.

Bin Wu (S'89–M'92–SM'99–F'08) received the Ph.D. degree in electrical and computer engineering from the University of Toronto, Toronto, ON, Canada, in 1993.

After being with Rockwell Automation Canada, he joined Ryerson University, Toronto, where he is currently a Professor and NSERC/Rockwell Industrial Research Chair in Power Electronics and Electric Drives. He has published more than 300 technical papers, authored/co-authored two Wiley-IEEE Press books, and holds more than 20 issued/pending patents in the area of power electronics, electric drives, and renewable energy systems.

Dr. Wu received the Gold Medal of the Governor General of Canada, the Premier's Research Excellence Award, Ryerson Distinguished Scholar Award, and the NSERC Synergy Award for Innovation. He is a Fellow of the Engineering Institute of Canada and the Canadian Academy of Engineering.

Venkata Yaramasu (S'08–M'14) was born in Karumanchi, Guntur, India. He received the B.Tech. degree in electrical and electronics engineering from Jawaharlal Nehru Technological University, Hyderabad, India, in 2005, the M.E. degree in electrical engineering with specialization in power electronics from the S. G. S. Institute of Technology and Science, Indore, India, in 2008, and the Ph.D. degree in electrical engineering from Ryerson University, Toronto, ON, Canada, in 2014.

He is currently a Postdoctoral Research Fellow at Ryerson University. His research interests include renewable energy, high-power converters, electric vehicles, and predictive control.

Dr. Yaramasu received six Best Student Paper Awards.

Zhongyuan Cheng (M'07) received the M.A.Sc. degree in electrical and computer engineering from Ryerson University, Toronto, ON, Canada, in 2005, and the Ph.D. degree in electrical engineering from the Huazhong University of Science and Technology, Wuhan, China.

In 2006, he joined Rockwell Automation, Cambridge, ON, Canada. He is currently working on medium-voltage drive topology, power electronics design, and motor drive control. His research interests include the integration and application aspects such as drive-utility interaction, MV drives in the generator system and drive stability in various applications, and design aspects such as pulse width modulation, power converter topology, and component sizing.

Navid Reza Zargari (S'91–M'95–SM'03) received the B.Eng. degree from Tehran University, Tehran, Iran in 1987, and the M.A.Sc. and Ph.D. degrees from Concordia University, Montreal, QC, Canada, in 1991 and 1995, respectively.

He has been with Rockwell Automation, Cambridge, ON, Canada, since November 1994, first as a Senior Designer and currently as the Manager of the Medium VOLTAGE R&D department. For the past 19 years, he has been involved with simulation, analysis, and design of power converters for medium-voltage ac drives. His research interests include power converter topologies and their control aspects, power semiconductors and renewable energy sources. He has co-authored more than 80 research papers and holds 20 US patents. In 2011, he co-authored a book on power conversion and control of wind energy systems.

Dr. Zargari is registered as a Professional Engineer in the Province of Ontario. He received the Premier's Innovation Award in 2009 from the Province of Ontario.